Supplementary Materials: Characterization and Photophysical Properties of a Luminescent Aluminum Hydride Complex Supported by a *β*-Diketiminate Ligand

Shunichiro Ito, Kazuo Tanaka and Yoshiki Chujo

NMR Spectra

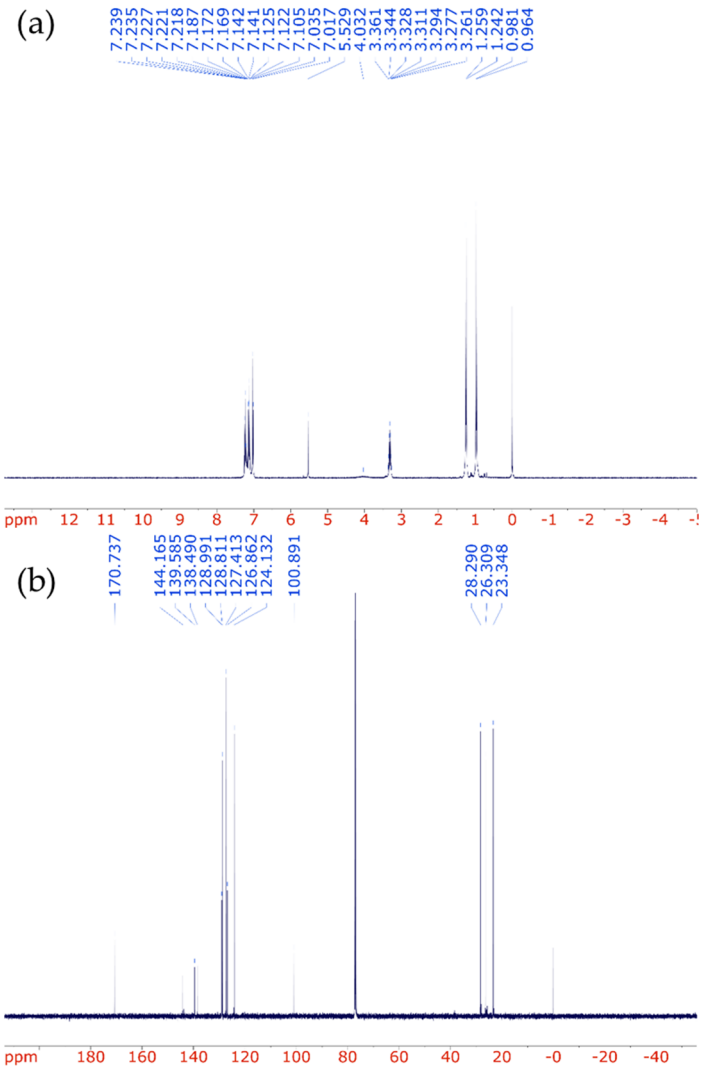

Figure S1. (**a**) ^{1}H and (**b**) ^{13}C{^{1}H} NMR spectra of **LAlH** in $CDCl_3$.

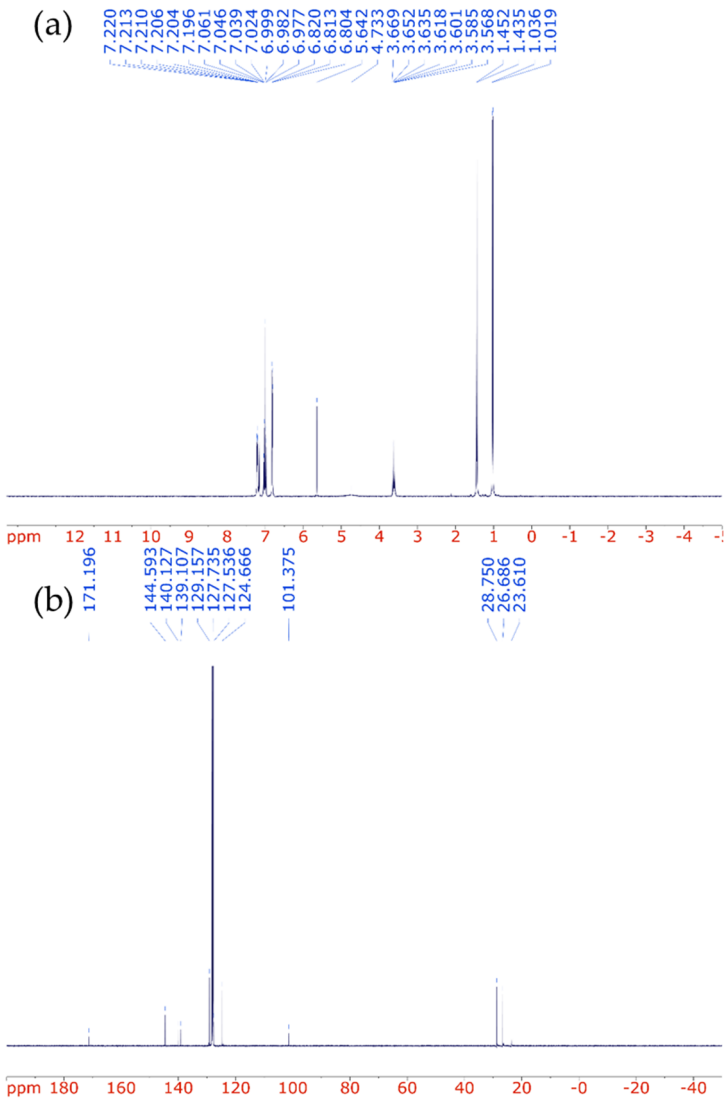

Figure S2. (**a**) ^{1}H and (**b**) $^{13}C\{^{1}H\}$ NMR spectra of **LAlH** in C_6D_6.

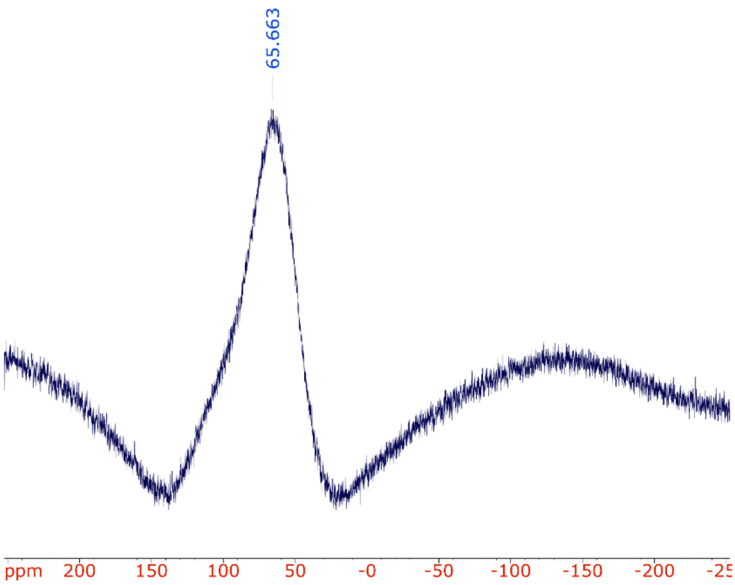

Figure S3. $^{27}Al\{^{1}H\}$ NMR spectrum of **LAlH** in C_6D_6. $Al(NO_3)_3{\cdot}9H_2O$ in D_2O was used as an external standard (0 ppm).

Single Crystal X-ray Analysis

Table S1. Selected X-ray data, collection and refinement parameters for **LAlH.**

Crystal data	
Chemical formula	$C_{39}H_{47}AlN_2$
M_r	570.76
Crystal system, Space group	Orthorhombic, *Pbca*
Temperature (K)	88
a, b, c (Å)	16.0206 (3), 24.7785 (5), 16.9022 (4)
V (Å^3)	6709.6 (2)
Z	8
Radiation type	Mo $K\alpha$
μ (mm^{-1})	0.09
Crystal size (mm)	0.70 × 0.30 × 0.25
Data collection	
Diffractometer	Rigaku Raxis Rapid
Absorption correction	Empirical (using intensity measurements) *ABSCOR*, (Rigaku, 1995)
T_{min}, T_{max}	0.861, 1.000
No. of measured, independent and observed [$I > 2\sigma(I)$] reflections	101680, 7680, 6542
R_{int}	0.044
(sin $\theta/\lambda)_{max}$ (Å^{-1})	0.649
Refinement	
$R[F^2 > 2\sigma(F^2)]$, $wR(F^2)$, S	0.043, 0.106, 1.05
No. of reflections	7680
No. of parameters	393
H-atom treatment	H atoms treated by a mixture of independent and constrained refinement
$\Delta\rho_{max}$, $\Delta\rho_{min}$ (e Å^{-3})	0.36, −0.21

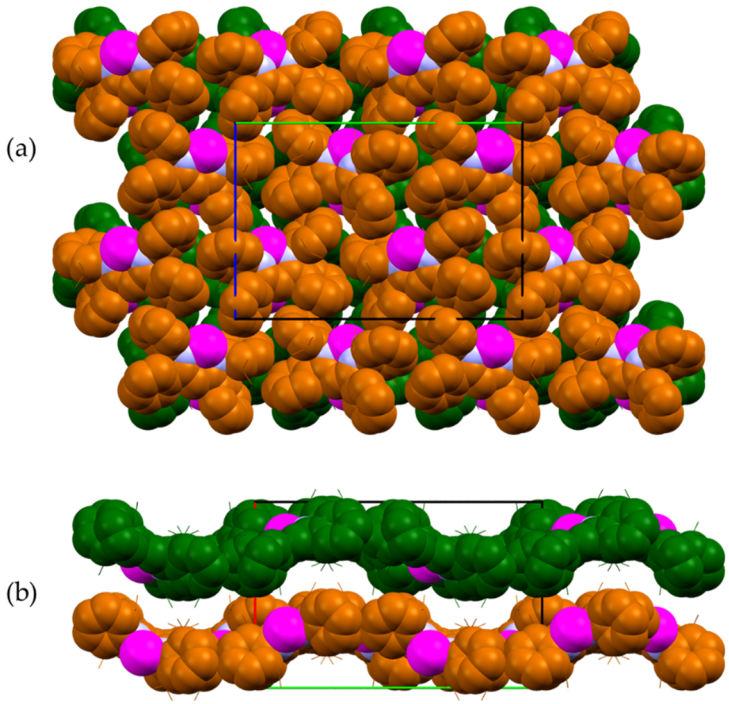

Figure S4. Packing diagram of **LAlH** viewed along with (a) *a* and (b) *b* axes. All hydrogen atoms were omitted for clarity. Isopropyl groups were shown in wireframe. Legends: red bar, *a* axis; green bar, *b* axis; and blue bar, *c* axis. Key to atom color: carbon, copper and green; aluminum, magenta; and nitrogen, blue.

Photophysical Measurements

Estimation of k_{FL}^0

First, the absorption band $\varepsilon(\lambda)$ in the longest wavelength region (361.5–543.5 nm) was fitted with a single-component Gaussian function as a function of wavelength:

$$\epsilon(\lambda) = \epsilon_0 + \frac{A}{w\sqrt{\pi/2}} \exp\left[-2\left(\frac{\lambda - \lambda_0}{w}\right)^2\right], \quad \text{(S1)}$$

where ε_0, λ_0, A and w were fitting parameters corresponding to a baseline, a central wavelength, an area, and a full width at half maximum, respectively. We converted the fitted curve in the wavelength scale to the one in the wavenumber scale by simply taking a reciprocal (Figure S5). The integration of the fitted curve was carried out, then the k_{FL}^0 value was estimated according to the Strickler–Berg equation:

$$k_{\mathrm{FL}}^0 = 2.880 \times 10^{-9} n^2 \, \tilde{\nu}_0^{\,2} \, \frac{g_l}{g_u} \int \epsilon(\tilde{\nu}) \, d\tilde{\nu}, \quad \text{(S2)}$$

where n means a refractive index of solvent, $\tilde{\nu}_0$ denotes photon energy in wavenumber at an absorption maximum, g_l and g_u are degeneracies of lower and upper states of interest, and $\epsilon(\tilde{\nu})$ is molar absorption coefficient as a function of wavenumber, respectively. The fitted parameters and the used values for the calculation were listed in Tables S2 and S3.

Table S2. Fitted parameters for the UV–vis spectrum.

Parameter	Fitted Value	Standard Error
ε_0	0.01254	0.00149
λ_0	394.21554	0.05969
w	49.27002	0.14788
A	85.50728	0.26228

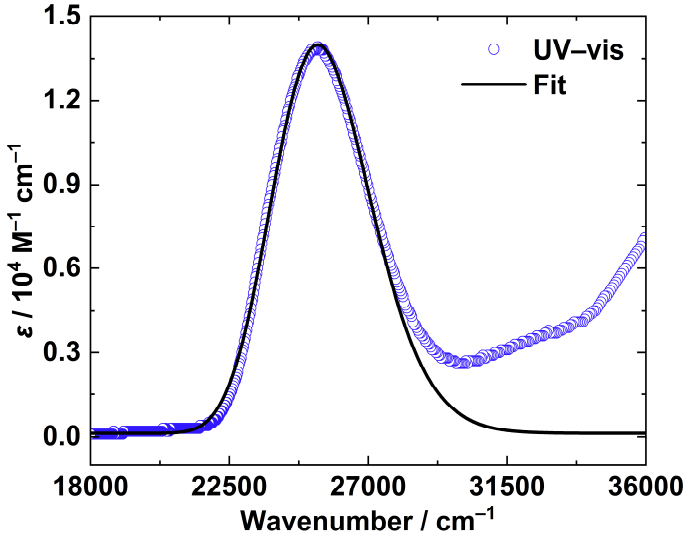

Figure S5. UV–vis absorption spectrum (blue circles) and the fitted curve (black line).

Table S3. Parameters for estimation of k_{FL}^0.

$\int \epsilon(\tilde{\nu}) \, d\tilde{\nu} \, / \mathrm{M^{-1}cm^{-2}}$	n	$\tilde{\nu}_0 \, / \mathrm{cm^{-1}}$
5.57×10^7	1.371	2.54×10^4

Fluorescence Lifetime

Fluorescence decay curves were recorded by using time-correlated single-photon counting method. Photoexcitation was carried out at 375 nm and instrument response functions (IRFs) were detected at 375 nm with a neutral density filter.

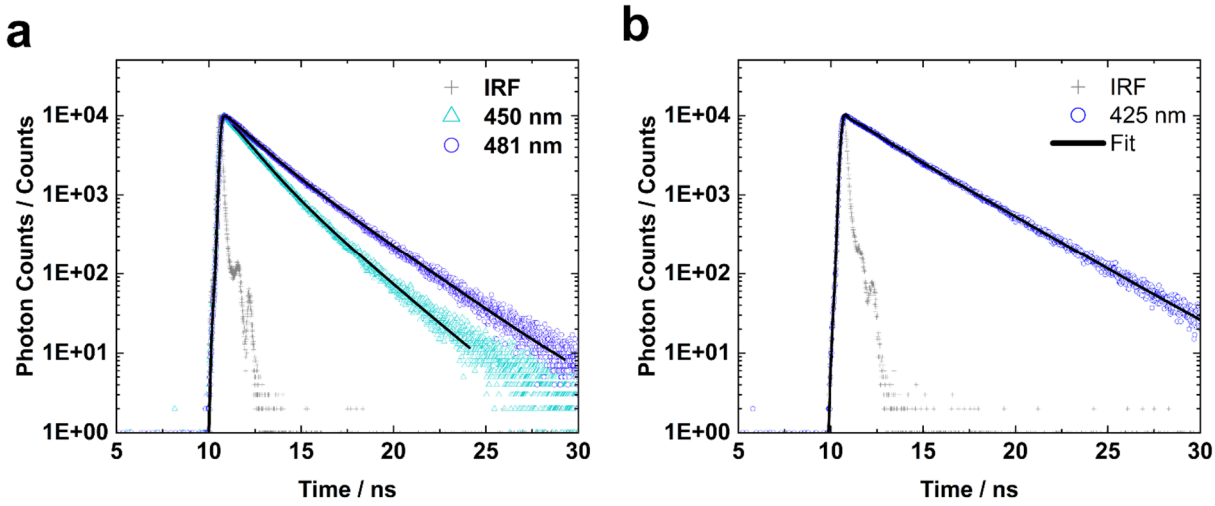

Figure S6. Fluorescence decay curves of **LAlH** (**a**) in the crystalline state at r.t. detected at 450 (cyan triangles) and 481 nm (blue circles) and (**b**) in the solution state at 80 K. Fitted curves were shown as solid lines.

Table S4. Fitted parameters for fluorescence lifetime measurements of the crystals at r.t.

	Detector Position	τ_1 / ns f_1 (%) [a]	τ_2 / ns f_2 (%) [a]	χ^2 [b]	$\langle\tau\rangle$ / ns [c]
Solution	425 nm	1.43 [d] 7.72 [d]	3.27 [d] 87.32 [d]	1.20	3.0
Crystal	450 nm	1.16 48.15	2.25 51.85	0.98	1.7
	481 nm	1.39 31.07	2.75 68.93	1.01	2.3

[a] Photoluminescence decay curve was fitted with two-exponential decay function: $I(t) = I_0 \Sigma \alpha_i \exp(-t/\tau_i)$. f_i's are fractions of each component i, which can be written as follows: $f_i = \alpha_i\tau_i / \Sigma \alpha_i\tau_i$. [b] Goodness-of-fit. [c] $\langle\tau\rangle = \Sigma \alpha_i\tau_i^2 / \Sigma \alpha_i\tau_i = \Sigma f_i\tau_i$. [d] Fitted by three-components exponential decay with one fixed component as scattered light (τ = 27.7 ps, f = 4.96%).

Kinetics of Photophysical Process

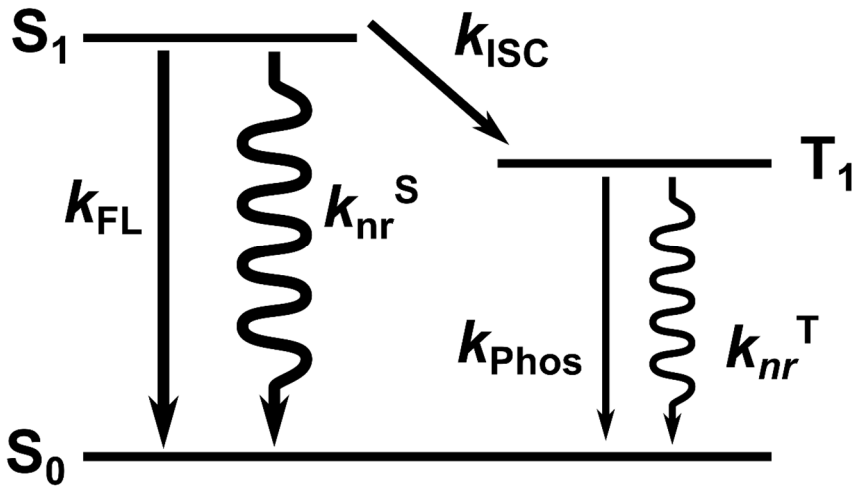

Figure S7. Simple Jablonski diagram for **LAlH**.

Phosphorescence Property

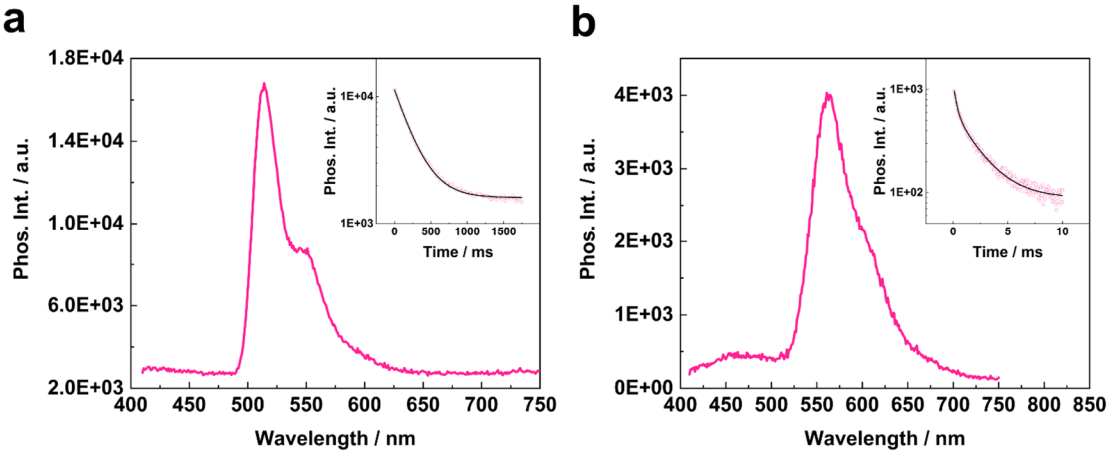

Figure S8. Phosphorescence spectra of **LAlH** at 80 K in (**a**) the solution and (**b**) crystalline states. The spectra were recorded after 1.0 ms from the excitation. Insets show the corresponding phosphorescence decay curves.

Table S5. Phosphorescence lifetimes of **LAlH** at 80 K.

Condition	τ_1 / ms A_1 / a.u.	τ_2 / ms A_2 / a.u.	R^2	$\langle\tau\rangle$ / ms [b]
Solution	231 9716	– [c] – [c]	0.999	231
Crystals	0.29 529	2.15 526	0.993	1.9

[a] Photoluminescence decay curve was fitted with exponential decay function: $I(t) = I_0 \Sigma A_i \exp(-t/\tau_i)$. [b] $\langle\tau\rangle = \Sigma A_i\tau_i^2 / \Sigma A_i\tau_i$. [c] Data were fitted with a single-component function.

Estimation of Fluorescence and Phosphorescence Quantum Yields

The photoluminescence spectrum of **LAlH** in the solution state at 80 K was deconvoluted with 7 Gaussian functions in wavelength scale, then the integrated intensities were calculated for both the fluorescence and the phosphorescence parts (Figure S9).

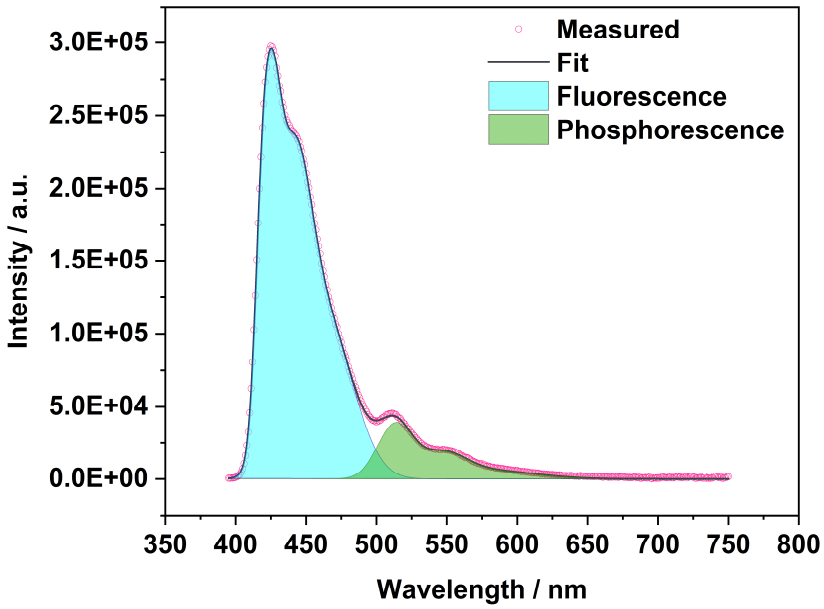

Figure S9. Deconvoluted photoluminescence spectrum of **LAlH** in the solution state at 80 K.

Table S6. Results of deconvolution of the photoluminescence spectrum.

Component	Integrated Intensity / a.u.	Intensity Ratio	Φ
Fluorescence	1.44×10^7	0.867	0.80
Phosphorescence	2.22×10^6	0.133	0.12

DFT Calculations

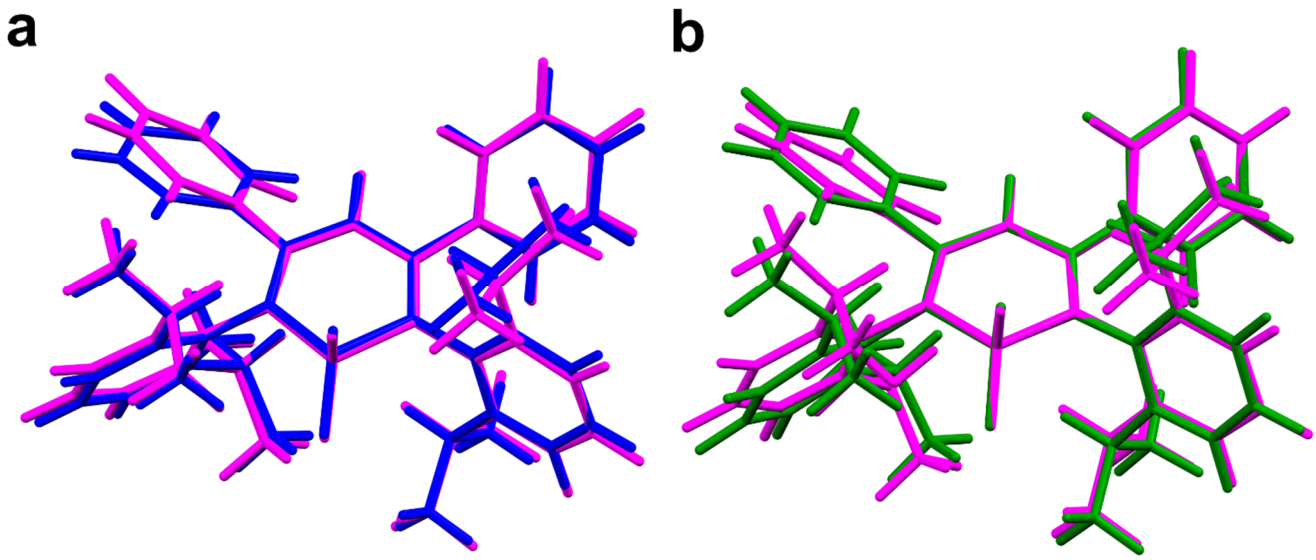

Figure S10. Superimposed structures of (**a**) the single-crystal (blue) and the S_0 optimized (magenta) structures, and (**b**) S_0 (magenta) and S_1 (green) optimized structures.

Calculation of Huang–Rhys Factors

We briefly overview the derivatization of internal conversion rate constant, according to the formalization by Lin [1]. When we regard a molecule without strong coupling with the neighboring molecules, *e.g.*, in a dilute solution, we can take the Hamiltonian for the system as follows;

$$\hat{H} = \hat{T} + \hat{h}_s + \sum_{\alpha} \hat{h}_\alpha + \sum_{\alpha>\beta} \hat{V}_{\alpha,\beta} + \sum_{\alpha} \hat{V}_{s,\alpha}, \tag{S3}$$

where where $\hat{\mathrm{T}}$ is the kinetic-energy operator of all nuclear motion including both intra- and intermolecular vibration of the solute and solvent molecules, h_s and $\sum_\alpha \hat{h}_\alpha$ are the electronic-energy operators for the internal state of the solute and solvent molecules, respectively, and $\sum_{\alpha>\beta} \hat{V}_{\alpha,\beta}$ and $\sum_\alpha \hat{V}_{s,\alpha}$, respectively, represent the potential energy of the solvent–solvent and the solute–solvent interactions. Using the adiabatic approximation, the state of the system, $|\Psi_{av}\rangle$, is described by the product of the wavefunctions for the electrons, $|\Phi_a\rangle$, and for the intra- and intermolecular vibrations, $|\Theta_{av}\rangle$:

$$|\Psi_{av}\rangle = |\Phi_a\rangle\,|\Theta_{av}\rangle\,. \tag{S4}$$

In this approximation, an electron does not make the transitions from one state to others. In other words, $|\Phi_a\rangle$, and $|\Theta_{av}\rangle$ are the solutions of the following Schrödinger equations:

$$\left(\hat{h}_s + \hat{h}_s + \sum_{\alpha} \hat{h}_\alpha + \sum_{\alpha>\beta} \hat{V}_{\alpha,\beta} + \sum_{\alpha} \hat{V}_{s,\alpha}\right) |\Phi_a\rangle = \hat{U}_a(\boldsymbol{R})\,|\Phi_a\rangle\,. \tag{S5}$$

and

$$\left[\hat{T} + \hat{U}_a(\boldsymbol{R})\right] |\Theta_{av}\rangle = E_{av}\,|\Theta_{av}\rangle\,, \tag{S6}$$

where $\hat{U}_a(\boldsymbol{R})$ is the adiabatic potential of the a-th electronic state at the instantaneous positions $\boldsymbol{R}$, and v signifies the overall vibrational state of the nuclei.

In order to consider the radiationless transitions, we must look for the perturbation causing the transition between different electronic states in accordance with the approximate nature of the wavefunctions given by Eq. S4. As shown by Huang and Rhys, and Kubo independently [2,3], the perturbation of the system for a process such as nonradiative transitions determined from the approximate nature of the wavefunction is given by

$$\hat{H}'\,|\Psi_{av}\rangle = \hat{T}\,|\Phi_a\rangle\,|\Theta_{av}\rangle - |\Phi_a\rangle\,\hat{T}\,|\Theta_{av}\rangle\,. \tag{S7}$$

We take the kinetic-energy operator of nuclear motion $\hat{\mathrm{T}}$ in terms of normal coordinates Q_i's including both intra- and intermolecular vibrations referring to the electronic state a:

$$\hat{T} = -\frac{1}{2}\hbar^2 \sum_i \frac{\partial^2}{\partial Q_i^2}, \tag{S8}$$

then the perturbation can be written as

$$\begin{aligned} \hat{H}'\,|\Psi_{av}\rangle &= -\frac{1}{2}\hbar^2 \sum_i \frac{\partial^2}{\partial Q_i^2}\,|\Phi_a\rangle\,|\Theta_{av}\rangle - |\Phi_a\rangle \left(-\frac{1}{2}\hbar^2 \sum_i \frac{\partial^2}{\partial Q_i^2}\right) |\Theta_{av}\rangle \\ &= -\hbar^2 \sum_i \left|\frac{\partial \Phi_a}{\partial Q_i}\right\rangle \left|\frac{\partial \Theta_{av}}{\partial Q_i}\right\rangle - \frac{1}{2}\hbar^2 \sum_i \left|\frac{\partial^2 \Phi_a}{\partial Q_i^2}\right\rangle |\Theta_{av}\rangle\,. \end{aligned} \tag{S9}$$

From time-dependent perturbation theory, the transition probability from the state (iv') to a final state (fv'') is

$$W\left(fv'' \to iv'\right) = \frac{2\pi}{\hbar} \left|\left\langle \Psi_{fv''} \left| \hat{H}' \right| \Psi_{iv'} \right\rangle\right|^2 \delta\left(E_{fv''} - E_{iv'}\right), \tag{S10}$$

where the quantities $E_{iv'}$ and $E_{fv''}$ are the energies of the system in the initial and final states, respectively. Since we assume that the vibrational relaxation time is much shorter than the electronic relaxation time, a general result will require a Boltzmann average of the transition probability over all thermally available vibrational states of the solute and solvent molecules. Hence, the total

transition probability is given by summing Eq. S10 over all initial vibrational states ν' wighted by their Boltzmann factors and then summing over all final vibrational states ν'' *c*onsistent with the energy conservation:

$$W(f \to i) = \frac{2\pi}{\hbar} \sum_{\nu'\nu''} P_{\nu'} \left| \left\langle \Psi_{f\nu''} \left| \hat{H}' \right| \Psi_{i\nu'} \right\rangle \right|^2 \delta\left(E_{f\nu''} - E_{i\nu'}\right), \tag{S11}$$

where $P_{\nu'}$ is the Boltzmann weighting factor and is given by

$$\begin{aligned} P_{\nu'} &= \left[\sum_{\nu'} \exp\left(-\frac{E_{i\nu'}}{kT}\right)\right]^{-1} \exp\left(-\frac{E_{i\nu'}}{kT}\right) \\ &= \prod_{k}^{N} 2\sinh\left(\frac{\hbar\omega_k'}{2kT}\right) \exp\left[-\left(\nu_k' + \frac{1}{2}\right)\frac{\hbar\omega_k'}{kT}\right], \end{aligned} \tag{S12}$$

where N represents the total number of normal modes of vibrations including both intra- and intermoleculr vibrations.

From Eq. S7 we have the matrix elements for the perturbation factor due to the i-th vibrational mode as

$$\begin{aligned} \left\langle \Psi_{f\nu''} \left| \hat{H}_i' \right| \Psi_{i\nu'} \right\rangle = &-\hbar^2 \left\langle \Phi_f \Theta_{f\nu''} \left| \frac{\partial \Phi_i}{\partial Q_i} \frac{\partial \Theta_{i\nu'}}{\partial Q_i} \right\rangle \right. \\ &- \frac{\hbar^2}{2} \left\langle \Phi_f \Theta_{f\nu''} \left| \Theta_{i\nu'} \frac{\partial^2 \Phi_i}{\partial Q_i^2} \right\rangle \right. . \end{aligned} \tag{S13}$$

When we apply the Condon approximation, Eq. S13 becomes

$$\left\langle \Psi_{f\nu''} \left| \hat{H}_i' \right| \Psi_{i\nu'} \right\rangle = R_i(fi) \left\langle \Theta_{f\nu''} \left| \frac{\partial}{\partial Q_i} \right| \Theta_{i\nu'} \right\rangle, \tag{S14}$$

where

$$R_i(fi) = -\hbar^2 \left\langle \Phi_f \left| \frac{\partial}{\partial Q_i} \right| \Phi_i \right\rangle. \tag{S15}$$

Thus, we find

$$W_{f\to i} = \frac{2\pi}{\hbar} \sum_{l} \sum_{\nu',\nu'' \neq l}' P_{\nu'} \left| R_l(fi) \right|^2 \left| \left\langle \Theta_{f\nu''} \left| \frac{\partial}{\partial Q_l} \right| \Theta_{i\nu'} \right\rangle \right|^2 \delta\left(E_{f\nu''} - E_{i\nu'}\right). \tag{S16}$$

Assuming only one promoting mode l, the rate constant of internal conversion becomes

$$W_{f\to i} = \frac{2\pi}{\hbar} \left| R_l(fi) \right|^2 \sum_{\nu',\nu'' \neq l}' P_{\nu'} \left| \left\langle \Theta_{f\nu''} \left| \frac{\partial}{\partial Q_l} \right| \Theta_{i\nu'} \right\rangle \right|^2 \delta\left(E_{f\nu''} - E_{i\nu'}\right). \tag{S17}$$

Considering that the potential energy surface for the excited state is assumed to be the same as that for the ground state except for a rigid displacement in the normal-mode coordinate, Eq. 17 can be reduced as follows [4–8]:

$$W_{f\to i} = \frac{1}{\hbar^2} \left(\frac{\omega_l}{2\hbar} \left| R_l(fi) \right|^2 \right) \sqrt{\frac{2\pi}{\sum_j' S_j \omega_j^2 \left(2\bar{n}_j + 1\right)}} \exp\left[-\frac{\left(\omega_{fi} + \omega_l + \sum_j' S_j \omega_j\right)^2}{2\sum_j' S_j \omega_j^2 \left(2\bar{n}_j + 1\right)} \right], \tag{S18}$$

where $\hbar\omega_{\mathrm{fi}}$ is the energy gap between the final state and the initial state, S_j is the Huang–Rhys factor for the j-th mode, $\sum_j' S_j \omega_j$ is the sum of the relaxation energies for all modes except the promoting mode l, $\bar{n}_j$ is the Boltzmann averaged number of phonon for j-th mode. The Huang–Rhys factor S_j is obtained as

$$S_j = \frac{\left(\omega_j \Delta Q_j\right)}{2\hbar}, \tag{S19}$$

where ΔQ_j is obtained from the gradient of the excited state energy (E^{exc}):

$$\Delta Q_j = \frac{1}{\omega_j^2}\frac{\partial E^{\mathrm{exc}}}{\partial Q_j}. \tag{S20}$$

Optimized Structures

Table S7. Optimized geometry of **LAlH** at the S_0 state.

Low Frequencies / cm^{-1}: −2.2799 −1.0016 −0.001 −0.0006 0.0009 1.0367 15.2521 28.8 33.1661

Center Number	Atomic Number	Coordinates (Angstroms)		
		x	y	z
1	13	0.001968	−1.38995	−0.88014
2	1	0.143758	−2.78146	−0.13427
3	1	−0.19394	−1.40489	−2.45939
4	7	1.466383	−0.23185	−0.37643
5	6	1.249891	1.06439	−0.14561
6	6	−0.02757	1.644683	−0.08189
7	1	−0.04051	2.716578	0.043738
8	7	−1.42771	−0.31002	−0.15193
9	6	−1.28378	1.006462	−0.02537
10	6	3.411206	2.140809	−0.86236
11	1	3.406225	1.514826	−1.74485
12	6	2.384649	2.016877	0.075484
13	6	4.425089	3.073612	−0.68169
14	1	5.211482	3.162525	−1.42429
15	6	4.432133	3.890254	0.445692
16	1	5.227587	4.61444	0.589441
17	6	3.411867	3.776276	1.384614
18	1	3.408083	4.409138	2.266303
19	6	2.390387	2.851163	1.195833
20	1	1.595155	2.765653	1.929137
21	6	−2.44465	1.932037	0.188506
22	6	−3.42031	1.712954	1.163798
23	1	−3.37917	0.827914	1.782729
24	6	−4.45032	2.627763	1.35363
25	1	−5.19406	2.441138	2.121493
26	6	−4.53062	3.771072	0.56512
27	1	−5.33894	4.480264	0.711575
28	6	−3.5682	3.996704	−0.41401
29	1	−3.62317	4.880347	−1.04161
30	6	−2.53242	3.087963	−0.5959
31	1	−1.79199	3.267089	−1.36807
32	6	2.769431	−0.8209	−0.17275
33	6	3.243803	−1.01818	1.140573
34	6	4.488471	−1.623	1.312937
35	1	4.867712	−1.77931	2.317386
36	6	5.244663	−2.04448	0.229907
37	1	6.210319	−2.51474	0.38667
38	6	4.749894	−1.87411	−1.05327
39	1	5.335317	−2.21982	−1.89902
40	6	3.513463	−1.26939	−1.28218
41	6	−2.70567	−0.97257	−0.05454
42	6	−2.97394	−1.7534	1.089571
43	6	−4.20467	−2.4036	1.174003
44	1	−4.43276	−2.99518	2.054913
45	6	−5.13896	−2.31725	0.152711
46	1	−6.09132	−2.83118	0.237415
47	6	−4.83892	−1.58577	−0.98541
48	1	−5.56128	−1.54128	−1.794

49	6	−3.62593	−0.90868	−1.12032
50	6	2.424497	−0.67492	2.376895
51	1	1.579482	−0.05467	2.072296
52	6	1.847015	−1.95642	2.995817
53	1	1.263455	−2.52087	2.264915
54	1	1.199313	−1.71476	3.845364
55	1	2.649184	−2.60723	3.358886
56	6	3.219523	0.116937	3.422172
57	1	4.017325	−0.48621	3.865819
58	1	2.558825	0.428378	4.237627
59	1	3.673637	1.011188	2.988933
60	6	3.012848	−1.15274	−2.71606
61	1	2.116906	−0.52664	−2.71497
62	6	2.614172	−2.53173	−3.26332
63	1	3.487907	−3.1887	−3.32758
64	1	2.184484	−2.43536	−4.265
65	1	1.87247	−3.0221	−2.62903
66	6	4.035409	−0.50163	−3.65856
67	1	4.379996	0.469614	−3.29357
68	1	3.588763	−0.3516	−4.64608
69	1	4.918784	−1.13305	−3.79272
70	6	−1.97984	−1.92389	2.232306
71	1	−1.05551	−1.41384	1.95276
72	6	−1.64326	−3.40454	2.456354
73	1	−2.5222	−3.96817	2.784308
74	1	−0.87884	−3.50535	3.232499
75	1	−1.26254	−3.86433	1.542003
76	6	−2.47834	−1.29631	3.542395
77	1	−2.64643	−0.22022	3.449486
78	1	−1.73967	−1.44712	4.335941
79	1	−3.41643	−1.75481	3.871189
80	6	−3.35478	−0.16342	−2.41989
81	1	−2.40174	0.360522	−2.32425
82	6	−3.21568	−1.14156	−3.59559
83	1	−2.41229	−1.85985	−3.42068
84	1	−2.98538	−0.59487	−4.51574
85	1	−4.14553	−1.69589	−3.75926
86	6	−4.43935	0.879942	−2.72261
87	1	−5.40039	0.40309	−2.93923
88	1	−4.16043	1.466801	−3.60357
89	1	−4.58536	1.567842	−1.88723

Table S8. Optimized geometry of **LAlH** at the S_1 state.

Low Frequencies / cm^{-1}: −0.0013 −0.0011 −0.0008 1.2969 1.851 2.621 10.9357 25.6479 32.5637

Center Number	Atomic Number	Coordinates (Angstroms)		
		x	y	z
1	13	0.014287	−1.38591	−0.789451
2	1	0.18062	−2.785505	−0.071401
3	1	−0.2787	−1.355357	−2.357984
4	7	1.486005	−0.239718	−0.394047
5	6	1.275097	1.103218	−0.220406
6	6	−0.035511	1.63929	−0.116389
7	1	−0.053932	2.716641	−0.052782
8	7	−1.424217	−0.329165	−0.042392
9	6	−1.320278	1.032386	−0.015168
10	6	3.50807	1.935171	−1.016493
11	1	3.5785	1.084639	−1.680414
12	6	2.382906	2.075431	−0.185283
13	6	4.516853	2.886792	−1.022376
14	1	5.366817	2.757513	−1.685172
15	6	4.442002	4.005006	−0.1934

16	1	5.234784	4.74576	−0.197524
17	6	3.338078	4.158036	0.640976
18	1	3.268438	5.017069	1.301043
19	6	2.324507	3.208649	0.64682
20	1	1.49012	3.333056	1.329313
21	6	−2.456028	1.945876	0.203062
22	6	−3.525713	1.63059	1.061756
23	1	−3.555436	0.672467	1.561609
24	6	−4.547212	2.539927	1.298692
25	1	−5.351286	2.268011	1.975388
26	6	−4.546634	3.789258	0.682293
27	1	−5.350093	4.494581	0.866759
28	6	−3.502111	4.116255	−0.179166
29	1	−3.49085	5.077977	−0.682532
30	6	−2.47601	3.212473	−0.415012
31	1	−1.695391	3.480594	−1.11884
32	6	2.736599	−0.838708	−0.053583
33	6	3.208453	−0.794011	1.28201
34	6	4.405116	−1.438684	1.584021
35	1	4.7697	−1.422593	2.605975
36	6	5.128069	−2.124612	0.618397
37	1	6.057143	−2.621028	0.879929
38	6	4.646535	−2.178577	−0.680314
39	1	5.211101	−2.717728	−1.434128
40	6	3.457904	−1.548251	−1.043827
41	6	−2.662449	−1.024888	−0.067542
42	6	−2.912404	−1.944025	0.985791
43	6	−4.110947	−2.653009	0.980034
44	1	−4.324616	−3.341555	1.791034
45	6	−5.040542	−2.489038	−0.036551
46	1	−5.969752	−3.049987	−0.022863
47	6	−4.770041	−1.613609	−1.080098
48	1	−5.488253	−1.51535	−1.88758
49	6	−3.592255	−0.873515	−1.128494
50	6	2.412693	−0.183323	2.427244
51	1	1.57219	0.373631	2.012522
52	6	1.825077	−1.292205	3.314029
53	1	1.227384	−1.995225	2.72762
54	1	1.186064	−0.861082	4.091844
55	1	2.618584	−1.861816	3.808257
56	6	3.239699	0.799731	3.265005
57	1	4.05255	0.294312	3.795268
58	1	2.604911	1.274971	4.019699
59	1	3.676664	1.58496	2.643872
60	6	3.005825	−1.629471	−2.496017
61	1	2.15689	−0.953306	−2.623142
62	6	2.530834	−3.045651	−2.852163
63	1	3.356433	−3.761727	−2.782546
64	1	2.14484	−3.071396	−3.87596
65	1	1.73753	−3.389277	−2.183919
66	6	4.096918	−1.181275	−3.479436
67	1	4.471614	−0.18008	−3.249302
68	1	3.696364	−1.164395	−4.497574
69	1	4.951997	−1.863896	−3.475029
70	6	−1.959263	−2.117615	2.159874
71	1	−1.034916	−1.591432	1.9156
72	6	−1.606167	−3.588187	2.408885
73	1	−2.47766	−4.166363	2.73174
74	1	−0.8541	−3.662706	3.200635
75	1	−1.198479	−4.053918	1.509066
76	6	−2.522546	−1.479003	3.438783
77	1	−2.707818	−0.408949	3.312914
78	1	−1.813403	−1.599638	4.263827
79	1	−3.464778	−1.951569	3.734952
80	6	−3.330496	−0.011282	−2.354653
81	1	−2.389928	0.522012	−2.207916

82	6	−3.164477	−0.884361	−3.608152
83	1	−2.361669	−1.613485	−3.481396
84	1	−2.92052	−0.257937	−4.47215
85	1	−4.088107	−1.425255	−3.837838
86	6	−4.435415	1.030759	−2.577492
87	1	−5.387446	0.551348	−2.826482
88	1	−4.169342	1.683695	−3.414553
89	1	−4.591438	1.655029	−1.695842

Electronic Transitions

Table S9. Result of TD-DFT calculation for **LAlH** at the S_0 geometry.

Excited State	Energy / eV	Wavelength / nm	*f*	Composition	Coefficient
1	3.5725	347.05	0.4205		
				HOMO -> LUMO	0.68764
2	4.5125	274.76	0.0302		
				HOMO-4 -> LUMO	0.17965
				HOMO-1 -> LUMO	0.63718
3	4.6946	264.1	0.1044		
				HOMO-4 -> LUMO	0.58276
				HOMO-3 -> LUMO	0.15636
				HOMO-2 -> LUMO	−0.21328
				HOMO-1 -> LUMO	−0.17943
4	5.0029	247.83	0.0023		
				HOMO-4 -> LUMO	0.14193
				HOMO-3 -> LUMO	0.27789
				HOMO-2 -> LUMO	0.50349
				HOMO-2 -> LUMO+2	−0.10187
				HOMO-2 -> LUMO+17	0.11441
				HOMO-1 -> LUMO+15	0.13189
5	5.0485	245.59	0.0186		
				HOMO-4 -> LUMO	−0.23696
				HOMO-4 -> LUMO+11	0.10964
				HOMO-3 -> LUMO	0.52714
				HOMO-2 -> LUMO	−0.22196
6	5.1426	241.09	0.0706		
				HOMO-8 -> LUMO	-0.17543
				HOMO-8 -> LUMO+4	0.11995
				HOMO-7 -> LUMO	0.21432
				HOMO-7 -> LUMO+2	0.17719
				HOMO-6 -> LUMO	0.24025
				HOMO-5 -> LUMO	0.4102
				HOMO-5 -> LUMO+4	0.11136
				HOMO-4 -> LUMO+4	−0.10515
7	5.1741	239.62	0.0405		
				HOMO-8 -> LUMO	−0.12651
				HOMO-8 -> LUMO+2	−0.12703
				HOMO-8 -> LUMO+7	−0.10842
				HOMO-7 -> LUMO	0.35163
				HOMO-6 -> LUMO	−0.11684
				HOMO-6 -> LUMO+2	0.15507
				HOMO-5 -> LUMO	−0.27419
				HOMO-5 -> LUMO+4	0.10604
				HOMO -> LUMO+2	−0.21677
				HOMO -> LUMO+4	0.14914
8	5.1882	238.97	0.0338		

				HOMO-8 -> LUMO	−0.15994
				HOMO-7 -> LUMO	−0.15358
				HOMO-7 -> LUMO+2	0.10618
				HOMO-6 -> LUMO	0.30303
				HOMO-6 -> LUMO+2	−0.18771
				HOMO-5 -> LUMO	−0.24322
				HOMO-5 -> LUMO+7	−0.13398
				HOMO-2 -> LUMO	−0.13938
				HOMO-1 -> LUMO+7	0.11772
				HOMO -> LUMO+2	−0.28678
9	5.2226	237.4	0.0589		
				HOMO-6 -> LUMO	0.1927
				HOMO-5 -> LUMO	−0.37032
				HOMO-2 -> LUMO	0.11722
				HOMO -> LUMO+2	0.46562
10	5.2829	234.69	0.0207		
				HOMO-4 -> LUMO+11	−0.21033
				HOMO-4 -> LUMO+13	0.24298
				HOMO-3 -> LUMO	0.25721
				HOMO-3 -> LUMO+11	0.11939
				HOMO-3 -> LUMO+13	0.11751
				HOMO-3 -> LUMO+14	−0.12127
				HOMO-3 -> LUMO+15	−0.12431
				HOMO-3 -> LUMO+16	−0.1808
				HOMO -> LUMO+2	0.16059
				HOMO -> LUMO+11	−0.14276
				HOMO -> LUMO+13	0.17414
11	5.3441	232	0.0468		
				HOMO-8 -> LUMO	0.19723
				HOMO-3 -> LUMO	0.1082
				HOMO-2 -> LUMO	0.2483
				HOMO-2 -> LUMO+17	−0.17309
				HOMO-2 -> LUMO+19	0.11206
				HOMO-2 -> LUMO+20	0.11196
				HOMO-1 -> LUMO+2	0.15454
				HOMO-1 -> LUMO+12	−0.11634
				HOMO-1 -> LUMO+15	−0.22248
				HOMO -> LUMO+2	−0.20259
				HOMO -> LUMO+15	−0.11044
12	5.4084	229.24	0.1286		
				HOMO-8 -> LUMO	0.44386
				HOMO-7 -> LUMO	0.17758
				HOMO-6 -> LUMO	0.33161
				HOMO-2 -> LUMO	−0.13114
13	5.4686	226.72	0.0016		
				HOMO-7 -> LUMO	−0.11875
				HOMO -> LUMO+1	0.38884
				HOMO -> LUMO+4	0.38638
				HOMO -> LUMO+5	−0.27345
				HOMO -> LUMO+6	0.12886
				HOMO -> LUMO+7	0.11417
14	5.5509	223.36	0.0129		
				HOMO-9 -> LUMO	−0.27345
				HOMO -> LUMO+1	−0.17592
				HOMO -> LUMO+4	0.28169
				HOMO -> LUMO+6	0.19735

				HOMO -> LUMO+10	0.21384
				HOMO -> LUMO+11	−0.14795
				HOMO -> LUMO+12	−0.11788
				HOMO -> LUMO+14	−0.14181
				HOMO -> LUMO+16	−0.16111
				HOMO -> LUMO+17	−0.13233
				HOMO -> LUMO+18	0.18288
15	5.5799	222.2	0.026		
				HOMO-9 -> LUMO	−0.15459
				HOMO -> LUMO+4	−0.18252
				HOMO -> LUMO+6	0.14743
				HOMO -> LUMO+7	0.54221
				HOMO -> LUMO+17	−0.11648
16	5.6235	220.47	0.0485		
				HOMO-9 -> LUMO	0.43416
				HOMO-7 -> LUMO	−0.11073
				HOMO-6 -> LUMO	0.10077
				HOMO -> LUMO+6	0.15374
				HOMO -> LUMO+7	0.20542
				HOMO -> LUMO+11	−0.21733
				HOMO -> LUMO+12	−0.16464
				HOMO -> LUMO+13	−0.15193
				HOMO -> LUMO+15	0.12202
17	5.6665	218.8	0.008		
				HOMO-9 -> LUMO	0.3607
				HOMO -> LUMO+1	−0.11645
				HOMO -> LUMO+4	0.13011
				HOMO -> LUMO+9	0.15866
				HOMO -> LUMO+11	0.23613
				HOMO -> LUMO+12	0.18906
				HOMO -> LUMO+13	0.17216
				HOMO -> LUMO+14	−0.15881
				HOMO -> LUMO+15	−0.10423
				HOMO -> LUMO+16	−0.14088
				HOMO -> LUMO+17	−0.1543
18	5.7827	214.41	0.0153		
				HOMO-3 -> LUMO+13	0.1342
				HOMO-2 -> LUMO+11	0.12853
				HOMO-2 -> LUMO+12	0.13641
				HOMO-2 -> LUMO+14	−0.114
				HOMO-2 -> LUMO+15	0.15172
				HOMO-1 -> LUMO+7	0.12396
				HOMO-1 -> LUMO+17	−0.1378
				HOMO -> LUMO+12	0.11725
				HOMO -> LUMO+15	0.10076
				HOMO -> LUMO+16	0.26011
				HOMO -> LUMO+17	−0.18403
				HOMO -> LUMO+20	0.2127
19	5.8745	211.05	0.029		
				HOMO-3 -> LUMO+11	0.14086
				HOMO-3 -> LUMO+13	−0.15721
				HOMO-2 -> LUMO+15	0.13262
				HOMO -> LUMO+1	0.22965
				HOMO -> LUMO+4	−0.21035
				HOMO -> LUMO+7	−0.11278
				HOMO -> LUMO+9	−0.14277

				HOMO -> LUMO+11	−0.14517
				HOMO -> LUMO+14	−0.10278
				HOMO -> LUMO+18	0.216
				HOMO -> LUMO+19	0.11219
				HOMO -> LUMO+21	0.17665
20	5.9468	208.49	0.0011		
				HOMO-3 -> LUMO+11	−0.12876
				HOMO-3 -> LUMO+13	0.136
				HOMO-2 -> LUMO+2	0.114
				HOMO-2 -> LUMO+15	−0.12834
				HOMO-1 -> LUMO+7	−0.146
				HOMO -> LUMO+1	0.23388
				HOMO -> LUMO+4	−0.10227
				HOMO -> LUMO+12	0.15129
				HOMO -> LUMO+14	−0.17766
				HOMO -> LUMO+17	−0.18173
				HOMO -> LUMO+18	0.16023
				HOMO -> LUMO+19	0.14689
				HOMO -> LUMO+21	0.15952

Table S10. Result of TD-DFT calculation for **LAlH** at the S_1 geometry.

Excited State	Energy / eV	Wavelength / nm	*f*	Composition	Coefficient
1	3.0634	404.73	0.3807		
				HOMO -> LUMO	0.69035
2	3.9828	311.3	0.0804		
				HOMO-4 -> LUMO	0.18012
				HOMO-2 -> LUMO	−0.10827
				HOMO-1 -> LUMO	0.64545
				HOMO-1 -> LUMO+1	0.10673
3	4.1321	300.05	0.1355		
				HOMO-4 -> LUMO	−0.45159
				HOMO-2 -> LUMO	0.4596
				HOMO-1 -> LUMO	0.20361
4	4.5449	272.8	0.0545		
				HOMO-5 -> LUMO	−0.23441
				HOMO-4 -> LUMO	−0.31322
				HOMO-3 -> LUMO	0.41448
				HOMO-2 -> LUMO	−0.3645
5	4.5617	271.79	0.0079		
				HOMO-4 -> LUMO	0.32858
				HOMO-3 -> LUMO	0.50799
				HOMO-2 -> LUMO	0.29593
6	4.6642	265.82	0.1764		
				HOMO-5 -> LUMO	0.64105
				HOMO-4 -> LUMO	−0.1279
				HOMO-3 -> LUMO	0.16054
				HOMO-2 -> LUMO	−0.11213
7	4.8647	254.87	0.0261		
				HOMO-6 -> LUMO	0.322
				HOMO -> LUMO+1	0.56191
8	4.8982	253.12	0.0258		
				HOMO-8 -> LUMO	0.11695
				HOMO-7 -> LUMO	−0.23536
				HOMO-7 -> LUMO+1	−0.152
				HOMO-6 -> LUMO	0.4156
				HOMO-6 -> LUMO+1	0.13986
				HOMO-5 -> LUMO+5	0.12177

				HOMO-1 -> LUMO+5	0.12642
				HOMO -> LUMO+1	−0.32379
9	4.9294	251.52	0.0246		
				HOMO-8 -> LUMO	0.38417
				HOMO-8 -> LUMO+1	−0.2104
				HOMO-7 -> LUMO	0.39431
				HOMO-5 -> LUMO+4	−0.10997
				HOMO -> LUMO+4	0.11165
10	5.0573	245.16	0.1573		
				HOMO-9 -> LUMO+1	0.10367
				HOMO-8 -> LUMO	0.39801
				HOMO-7 -> LUMO	−0.36899
				HOMO-6 -> LUMO	−0.28703
				HOMO -> LUMO+1	0.14368
11	5.1384	241.29	0.0427		
				HOMO-8 -> LUMO	−0.11451
				HOMO-4 -> LUMO+11	0.11138
				HOMO-4 -> LUMO+14	0.10004
				HOMO-4 -> LUMO+15	−0.16787
				HOMO-2 -> LUMO	0.10139
				HOMO-2 -> LUMO+4	−0.1219
				HOMO-2 -> LUMO+11	0.10194
				HOMO-2 -> LUMO+15	0.16434
				HOMO-1 -> LUMO+14	−0.11188
				HOMO -> LUMO+4	0.30102
				HOMO -> LUMO+11	0.12316
				HOMO -> LUMO+15	−0.24995
12	5.2019	238.34	0.0191		
				HOMO-3 -> LUMO	−0.13583
				HOMO-3 -> LUMO+5	0.10875
				HOMO-3 -> LUMO+11	−0.14836
				HOMO-3 -> LUMO+17	0.13164
				HOMO-3 -> LUMO+18	0.11835
				HOMO-3 -> LUMO+20	0.13818
				HOMO-1 -> LUMO+1	−0.13545
				HOMO-1 -> LUMO+11	−0.18502
				HOMO-1 -> LUMO+14	0.29086
				HOMO-1 -> LUMO+15	0.12603
				HOMO -> LUMO+11	−0.18514
				HOMO -> LUMO+14	0.24703
13	5.2634	235.56	0.0044		
				HOMO-9 -> LUMO	0.64515
14	5.3503	231.73	0.0011		
				HOMO-2 -> LUMO+15	−0.1096
				HOMO -> LUMO+2	−0.29223
				HOMO -> LUMO+4	0.4166
				HOMO -> LUMO+5	0.25399
				HOMO -> LUMO+11	−0.10898
				HOMO -> LUMO+15	0.13004
15	5.4147	228.98	0.0167		
				HOMO -> LUMO+3	−0.19245
				HOMO -> LUMO+4	−0.14492
				HOMO -> LUMO+5	0.51985
				HOMO -> LUMO+6	−0.15424
				HOMO -> LUMO+7	0.16934
16	5.4371	228.03	0.1113		
				HOMO -> LUMO+2	0.14729
				HOMO -> LUMO+4	0.19113
				HOMO -> LUMO+10	−0.2739

				HOMO -> LUMO+11	0.36255
				HOMO -> LUMO+13	−0.14035
				HOMO -> LUMO+14	0.103
				HOMO -> LUMO+15	0.24042
17	5.5558	223.16	0.011		
				HOMO -> LUMO+2	0.4056
				HOMO -> LUMO+4	0.15591
				HOMO -> LUMO+5	0.10072
				HOMO -> LUMO+9	−0.16132
				HOMO -> LUMO+11	−0.21373
				HOMO -> LUMO+16	0.17741
				HOMO -> LUMO+20	0.19763
				HOMO -> LUMO+24	−0.11186
18	5.6772	218.39	0.0114		
				HOMO-4 -> LUMO+15	0.10378
				HOMO-3 -> LUMO+11	0.12106
				HOMO-3 -> LUMO+14	−0.18262
				HOMO-2 -> LUMO+11	−0.10202
				HOMO-1 -> LUMO+5	0.12199
				HOMO-1 -> LUMO+11	−0.1225
				HOMO -> LUMO+4	0.11382
				HOMO -> LUMO+5	−0.17115
				HOMO -> LUMO+14	0.12155
				HOMO -> LUMO+16	−0.18673
				HOMO -> LUMO+17	0.22611
				HOMO -> LUMO+18	0.19655
				HOMO -> LUMO+19	−0.18974
				HOMO -> LUMO+22	0.10492
19	5.8083	213.46	0.0205		
				HOMO-10 -> LUMO	−0.10419
				HOMO-6 -> LUMO	−0.12217
				HOMO-1 -> LUMO+1	0.2365
				HOMO-1 -> LUMO+5	0.13593
				HOMO -> LUMO+2	−0.20444
				HOMO -> LUMO+4	−0.11127
				HOMO -> LUMO+6	−0.10334
				HOMO -> LUMO+10	−0.10033
				HOMO -> LUMO+19	0.11112
				HOMO -> LUMO+20	0.19879
				HOMO -> LUMO+21	−0.12299
				HOMO -> LUMO+23	−0.18605
				HOMO -> LUMO+24	−0.12015
20	5.8596	211.59	0.0008		
				HOMO-10 -> LUMO	0.37473
				HOMO-7 -> LUMO	0.13442
				HOMO-6 -> LUMO	−0.10545
				HOMO-1 -> LUMO+1	−0.21311
				HOMO-1 -> LUMO+5	0.29834
				HOMO-1 -> LUMO+7	0.1102

References

1. Lin, S.H. Rate of Interconversion of Electronic and Vibrational Energy. *J. Chem. Phys.* **1966**, *44*, 3759–3767.
2. Huang, K.; Rhys, A. Theory of light absorption and non-radiative transitions in F -centres. *Proc. R. Soc. London. Ser. A. Math. Phys. Sci.* **1950**, *204*, 406–423.
3. Kubo, R. Thermal Ionization of Trapped Electrons. *Phys. Rev.* **1952**, *86*, 929–937.

4. Yu, G.; Yin, S.; Liu, Y.; Chen, J.; Xu, X.; Sun, X.; Ma, D.; Zhan, X.; Peng, Q.; Shuai, Z.; et al. Structures, Electronic States, Photoluminescence, and Carrier Transport Properties of 1,1-Disubstituted 2,3,4,5-Tetraphenylsiloles. *J. Am. Chem. Soc.* **2005**, *127*, 6335–6346.
5. Yin, S.; Peng, Q.; Shuai, Z.; Fang, W.; Wang, Y.-H.; Luo, Y. Aggregation-enhanced luminescence and vibronic coupling of silole molecules from first principles. *Phys. Rev. B* **2006**, *73*, 205409.
6. Peng, Q.; Yi, Y.; Shuai, Z.; Shao, J. Toward Quantitative Prediction of Molecular Fluorescence Quantum Efficiency: Role of Duschinsky Rotation. *J. Am. Chem. Soc.* **2007**, *129*, 9333–9339.
7. Peng, Q.; Niu, Y.; Wu, Q.; Gao, X.; Shuai, Z. Theoretical Understanding of AIE Phenomena Through Computational Chemistry. In *Aggregation-Induced Emission: Fundamentals*; John Wiley and Sons Ltd: Chichester, United Kingdom, 2013; pp. 357–398.
8. Jin, J.-L.; Geng, Y.; Su, Z.-M. Recent Theoretical Advances in Understanding the Mechanism of Aggregation-Induced Emission for Small Organic Molecules. In *Aggregation-Induced Emission: Fundamentals*; John Wiley and Sons Ltd: Chichester, United Kingdom, 2013; pp. 399–418.